Applied Surface Science 255 (2008) 1692–1698

Contents lists available at ScienceDirect

Applied Surface Science

journal homepage: www.elsevier.com/locate/apsusc

Laser cladding of SiC reinforced $Zr_{65}Al_{7.5}Ni_{10}Cu_{17.5}$ amorphous coating on magnesium substrate

T.M. Yue *, Y.P. Su

The Advanced Manufacturing Technology Research Centre, Department of Industrial and Systems Engineering, The Hong Kong Polytechnic University, Hung Hom, Hong Kong

ARTICLE INFO

Article history:
Received 23 November 2007
Received in revised form 11 April 2008
Accepted 5 June 2008
Available online 18 June 2008

PACS:
78.55.Qr
81.05.Ni
81.15.Fg

Keywords:
Laser cladding
Amorphous coating
Composite
Wear
Corrosion

ABSTRACT

$Zr_{65}Al_{7.5}Ni_{10}Cu_{17.5}$ amorphous coatings reinforced with SiC particles were fabricated on magnesium substrates using laser cladding with the aim of improving the inherently poor corrosion and wear properties of magnesium. The formation of a reaction layer containing ZrC between SiC particles and the matrix of the glassy phase did not show any significant effects on the thermal stability of the matrix. The wear resistance of the composite coating, measured in terms of volumetric loss, was 2–7 times, and 90 times higher than that of the unreinforced coating and the magnesium substrate respectively. Although the electrochemical stability of the composite coating was inferior to that of the unreinforced coating, it still displayed excellent corrosion resistance.

1. Introduction

Magnesium alloys, owing to their high strength-to-weight ratio, good castability and excellent machining properties are becoming important materials for applications in aerospace, transportation, military and sports equipment industries [1–3]. However, magnesium is one of the most active structural metals and cannot form self-healing passivating surface films in corrosive environments. Moreover, magnesium alloys usually have very low hardness and poor wear resistance, therefore can be easily worn down, especially under unlubricated friction conditions. Indeed, the poor inherent corrosion properties and poor wear resistance of magnesium alloys have seriously impeded the wider application of the alloys. In order to improve the corrosion and wear resistance of these magnesium alloys, surface modification technologies, such as electrochemical plating, conversion coatings, anodizing, gas-phase deposition processes, organic coating and high energy beam coating have been applied to them [4]. Notwithstanding the success of these techniques, they all have their own limitations. To date, it is still difficult to find a single coating technology capable of providing adequate protection from corrosion and abrasion for magnesium alloys, in harsh service environments.

Among the many surface engineering techniques, laser cladding has attracted much attraction in recent years. Its main advantage over other techniques is its ability to form a variety of relatively thick, tailor made, protective coatings. Also, it is a cleaner process than many of the chemical-based wet processes. Recently, there has been a growing interest in the laser cladding of glassy alloys onto light alloys, including magnesium, with the aim of improving their resistance to wear and corrosion [5–7]. The results so far show that when the substrate is coated with a layer of amorphous material, it becomes more resistant both to wear and to corrosion. Unfortunately, as is also well known, monolithic amorphous alloys themselves face the problem of low ductility. The typical plastic strain to failure for monolithic amorphous alloys, is normally less than two percent in compression and virtually zero in tension, at room temperature [8,9]. This is due mainly to the ease with which highly localized shear bands are formed. The fact is, although the local plastic strain in a single shear band can be quite large, only a few shear bands are active before failure. In order to improve the mechanical properties of these alloys, ceramic reinforcements were introduced into the glassy matrix to synthesize particulate reinforced amorphous matrix composites (PAMCs). These composites display enhanced strength, stiffness, plastic strain and impact

* Corresponding author. Tel.: +852 276 66601; fax: +852 236 25267.
E-mail address: mftmyue@inet.polyu.edu.hk (T.M. Yue).

0169-4332/$ – see front matter © 2008 Elsevier B.V. All rights reserved.
doi:10.1016/j.apsusc.2008.06.036

toughness when compared to the monolithic amorphous alloys [10–13]. But one should bear in mind that the introduction of a reinforcing phase into an amorphous matrix could cause a change in corrosion and wear properties.

Among the many amorphous alloys, Zr-based glassy alloys are good glass formers and can be cast in such a way as to produce bulk monolithic amorphous samples with a diameter of several centimetres [14]. One of the Zr-based alloys, the $Zr_{65}Al_{7.5}Ni_{10}Cu_{17.5}$ alloy, possesses excellent glass-forming ability. Its critical cooling rate for the formation of amorphous phase is only about 1.5 K/s [15]. Recently, magnesium substrates have been successfully cladded with Zr-based amorphous alloys [5]. Regarding the laser cladding of magnesium substrates with PAMC coatings, little information can be found in the literature. With this in mind, the present work studies the laser cladding of magnesium substrates with $Zr_{65}Al_{7.5}Ni_{10}Cu_{17.5}$ alloy reinforced with SiC particles. The scope of the study includes microstructural characterization and thermal stability analysis, as well as the evaluation of the wear behaviour and electrochemical properties of the material cladded.

2. Experimental approach

2.1. Laser cladding

Elemental metal powders with the nominal atomic percentage composition of $Zr_{65}Al_{7.5}Ni_{10}Cu_{17.5}$ were mixed with SiC particles using a ball mill, for 24 h in an Ar-gas atmosphere. The volume fraction of the SiC reinforcement phase in the composite material was 15%. The size of the SiC particle ranges from 50 μm to 74 μm, and the mean size is 60 μm. All the metal powders had a purity higher than 99.9 wt% and a mesh size of 200–300; while the magnesium substrate had a purity of 99.9 wt%. The laser cladding experiment was conducted on a magnesium substrate which had a surface area of 30 mm × 30 mm. The experiment was carried out using a laser rapid forming system consisting of a 5 kW continuous wave CO_2 laser, a four-axis numerical control working table and a powder feeder with a lateral nozzle. The experiment was conducted inside a glove box, where high-purity argon gas was continuously supplied at a flow rate of 25 l/min during the experiment to prevent the molten metal from oxidizing. The working principle of the system has been described previously [16]. The laser beam was directed onto the substrate to create a molten pool into which the premixed powders were injected through the powder feed nozzle, at a feed rate of 8.0 g per minute. This was to avoid the direct melting of the powder by the laser beam, as occurs in the two-step pre-placed [17], and powder bed re-melting methods [7]. The present one-step melting method yields a high quenching and cooling rate, and this prevents the formation of non-amorphous phases. In the present work, the focal diameter of the laser beam was 3 mm, the scanning rate was 5 mm/s and the laser power employed was 4.2 kW. On the magnesium substrate, five deposition tracks were produced with an overlapping percentage of 30%; two layers were deposited. The total thickness of the coating was about 1.8 mm.

2.2. Microstructural characterization

Specimens for the examination of microstructure were extracted from the coating at a depth of 0.5 mm. The microstructure of these specimens was examined by optical microscopy, scanning electron microscopy (SEM) together with energy dispersive X-ray spectroscopy (EDS), also using X-ray diffraction technique with Cu K_α radiation, and transmission electron microscopy (TEM). TEM specimens were obtained by electropolishing, using a twin jet polisher. A Philips EM 420 transmission electron microscope was employed for the study. Furthermore, transverse cross-sections of the coating were also prepared and analyzed. The composition within the interface region between the particles and matrix was measured by an electron probe microanalyzer (EPMA). The hardness value across the interface region was measured using a nano-hardness tester, which has a loading force capacity of 10 μN to 1 N and a resolution of 150 nN. Both the loading rate and the unloading rate of the hardness test were set at 20 mN/min. The loading force was continuously increased till the depth of the indentation reached 250 nm. The distance between two indentations was about six times the diagonal of the indent so as to avoid the effect of stress field. The thermal stability of the coating, in terms of the glass transition and crystallization temperatures, was examined using differential scanning calorimetry (DSC) at a heating rate of 0.17 K/s.

2.3. Wear and corrosion tests

The wear properties of the coating were investigated using a Sciland pin-on-disc tribometer. The specimens for the wear test have a surface area of 10 mm × 10 mm, and were tested under the loadings of 300 g, 600 g and 900 g at room temperature. The rotational speed of the disc was 150 rpm, and the total sliding time for the test was 1 h. The friction coefficient of the specimen was also measured during the test. The electrochemical behaviour of the coatings was evaluated using electrochemical impedance spectroscopy (EIS). A graphite rod was used as the counter electrode. The reference electrode was a standard calomel electrode (SCE). The test was performed in a 3.5 wt% NaCl solution at 25 °C. The specimens were ground with 800 grit emery paper, and cleaned with deionised water and alcohol. A sinusoidal voltage of 5 mV and a frequency range of 1×10^5 Hz to 1×10^{-2} Hz were employed. The test was conducted under open-circuit potential conditions.

3. Results and discussion

3.1. Microstructure

A cross-section of the coating, perpendicular to the direction of laser deposition, shows that the coating has a thickness of approximately 1.8 mm (Fig. 1), in which there are no cracks or voids. A metallurgical bond was obtained at the coating–substrate interface. Fig. 2 shows the distribution of elements measured by EDS across the substrate and coating. The distribution is reasonably uniform across the coating, except at the interface region

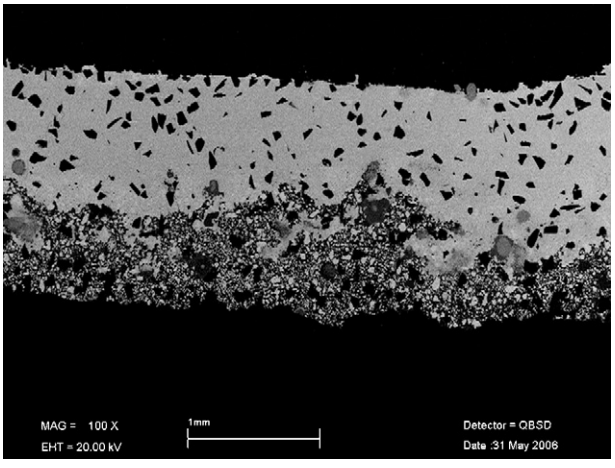

Fig. 1. A SEM micrograph showing a transverse cross-section of the coating.